

# Experimental study of the vibro-acoustics of a beam with periodically attached short bars

Zhenglong Gong,<sup>(1)</sup> Clancy Dawson,<sup>(1)</sup> Yanni Zhang,<sup>(2)</sup> David Matthews,<sup>(1,3)</sup> Hongmei Sun,<sup>(1)</sup> and Jie Pan<sup>(1)</sup>

<sup>(1)</sup> School of Mechanical and Chemical Engineering, The University of Western Australia, Perth, Australia

<sup>(2)</sup> School of Marine Science and Technology, Northwestern Polytechnical University, Xi'an, Shaanxi 710072, China

<sup>(3)</sup> DST, HMAS Stirling, Perth, Australia

## ABSTRACT

Periodic structures have well-known band-pass and band-stop frequency properties in wave propagation and sound radiation. However, little experimental research focusing on the performance of periodic attachments mounted by various interface materials and distributed structural elements has been undertaken. The aim of this research is to experimentally investigate the effects of lumped masses and short bars periodically attached to a long beam with various interface materials on the vibration transmission and noise radiation of the resulting periodic structure. The focus of this paper is to demonstrate that the band-pass and band-stop properties of the vibration and sound in the structure are dependent on the periodic arrangement and local resonance of the short bars, as well as the elastic bounding layer between the short bars and the long beam.

## 1 INTRODUCTION

The vibro-acoustics of periodic structures has been an intensive area of research as it has many practical applications in underwater acoustics and noise/vibration control of practical structures. Much work has been done in understanding the band-pass, band-gap, and energy-localization properties of structures with periodic point/line discontinuities, such as lumped masses and ribs.<sup>[1,2]</sup> Recent work by Zhang *et al.*<sup>[3][4]</sup> investigated the underwater sound absorption, reflection, and radiation by structures with periodically located distributed discontinuities. Distributed discontinuities, such as thin plates with finite length, affect the structural and sound waves, not only by scattering due to the finite size, but also by interaction between the wave and their own local resonance modes. In particular, distributed discontinuities can be placed on the surface or inside of an elastic coating layer,<sup>[4]</sup> which allows for extra mechanisms and parameters for optimal design of the acoustical surface

However, all the previous work on the vibro-acoustics of structures with periodically located distributed discontinuities was analytically or numerically based. Furthermore, the structures were infinitely long for the mathematical convenience of providing an ideal periodic structure. Although they were logical mathematically and numerically, some of the predicted results were still hard to comprehend based on common engineering sense. This paper presents work experimentally investigating the vibro-acoustics of a finite beam with periodic point and distributed discontinuities. The aims of this work are to (1) examine the general vibro-acoustical features of finite periodic structures and (2) check if some of the previous claims from analytical approaches were correct. Some preliminary experimental results are reported in this paper.

## 2 EXPERIMENTAL DESCRIPTION

In this research, periodic structures were investigated using two separate 4-m aluminium beams with width 40 mm and thickness 6 mm. One beam was left uncoated while the other was sprayed with a thin layer of rubber paint (Plastidip) on both sides. The first type of periodic structure (with point discontinuities) was obtained by attaching a number of small ferrite magnets (pass×36×6.5 mm) at regular intervals along the length of the beams. The magnets were placed in pairs on opposite sides of the bar to ensure secure contact through magnetic interaction. Two periodic spacings were investigated: 364 mm and 182 mm. The longer spacing resulted in eleven pairs of magnets uniformly arranged along the 4-m length whereas the shorter spacing had twenty-two pairs. The effect of the mass of the periodic structures was also investigated by attaching four magnets at each location for the longer 364-mm spacing. This resulted in the same periodic structure but with twice the mass at each location of contact. These configurations were made for both the plane aluminium beam and the rubber-coated beam. In addition to the magnets, one bar was prepared with short aluminium bars (182×40×3 mm) glued along the length of the beam with a spacing of 364 mm. A summary of the various configurations is given in Table 1.

Table 1. Summary of the various structural configurations used.

	SPACING (mm)	# ATTACHMENTS	# MAGNETS AT EACH POINT	# MAGNETS ON BEAM	TOTAL MASS MAGNETS (kg)
<b>Plain aluminium beam</b>					
<b>A</b>	364	11	2	22	1.144
<b>B</b>	182	22	2	44	2.288
<b>C</b>	364	11	4	44	2.288
<b>RUBBER-COATED ALUMINIUM BEAM</b>					
<b>D</b>	364	11	2	22	1.144
<b>E</b>	182	22	2	44	2.288
<b>F</b>	364	11	4	44	2.288
<b>PLAIN ALUMINIUM BEAM WITH SHORT ALUMINIUM BARS</b>					
<b>G</b>	364	11	-	-	

A diagram of the overall setup is shown in Figure 1. The aluminium beam was suspended horizontally from two attachment points 1.0 m from each end. The bars were excited by hitting one end (point A in Figure 1) using a B&K 8206 impact hammer with a metal head. A PCB 352C67 accelerometer was attached at the opposite end of the beam (point B in Figure 1). The frequency response functions (FRF) of the beams between points B and A were used to extract the vibration properties of the beam. The sound pressure and intensity were also measured perpendicular to the beam at a distance of 50 mm from the surface at the same location as that the accelerometer. This was done using a pair of microphones based on the FRFs  $H_1 = p_1 / F$  and  $H_2 = p_2 / F$  obtained by the impact method:

$$\frac{I_R}{F^2} = -\frac{1}{4\omega\rho_0\Delta x} \left| \frac{P_1}{F} \right| \left| \frac{P_2}{F} \right| \sin(\theta_2 - \theta_1), \quad (1)$$

where  $\theta_1$  and  $\theta_2$  are the phase angles of  $H_1$  and  $H_2$ ,  $p_1$  and  $p_2$  are the pressures measured by the microphones,  $F$  is the input force from the impact hammer, and  $\Delta x$  is the spacing between the microphones and set to 50 mm for all measurements as described below.

All data were collected using a Bruel & Kjaer 3050-B-060 data acquisition unit with a bandwidth of 3.2 kHz and a frequency resolution of 1 Hz. An average of ten impulses was used for each measurement. Case G is similar to Case A except that the ferrite magnets were replaced with short aluminium bars of dimensions 182x40x3 mm.

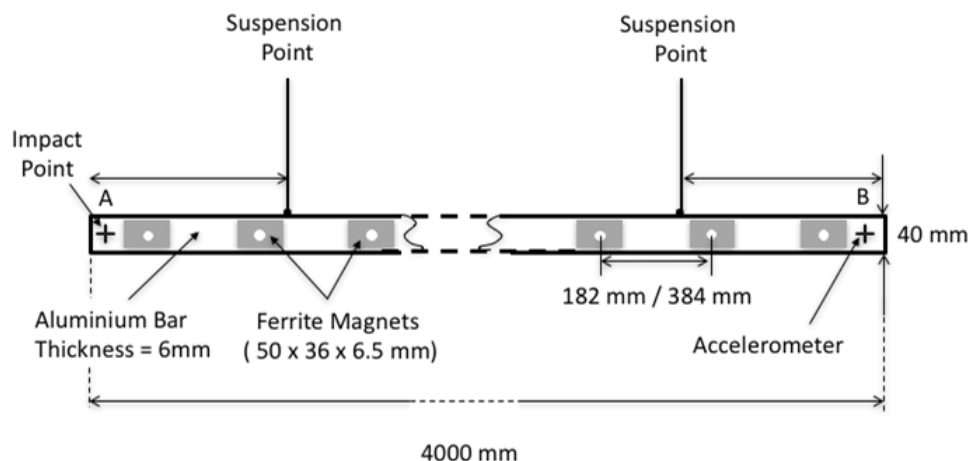


Figure 1. Experimental setup of the aluminium beam with ferrite magnets.

### 3 RESULTS AND DISCUSSION

#### 3.1 Plain aluminium beam and beam with periodic magnets

Figure 2(a) shows the FRFs of the raw aluminium beam and the beam coated in rubber paint. For frequencies less than 1000 Hz, there is little difference between them and even at higher frequencies only a slight attenuation is observed around 1400 Hz. Figure 2(b) shows the FRFs for the plain aluminium bar with eleven magnet pairs attached along the length with a spacing of 364 mm (Case A in Table 1). A clear 100-Hz-wide minimum is observed around 350 Hz, indicative of a band gap where there is a significant drop in the response by up to 30 dB. Interestingly, around 100 Hz, there also appears to be a band pass where there is a 10-dB increase in the response. In order to investigate these features further, the FRFs were measured for Cases B and C. In Case C, the spacing of the magnets was kept the same as in Case A, but instead of having two magnets at each point there are now four. This increases the mass at each attachment point from 0.104 kg to 0.208 kg and increases the total mass loading of the beam from 1.144 kg to 2.288 kg. A comparison of the FRFs for this configuration compared to Case A is shown in Figure 3(a).

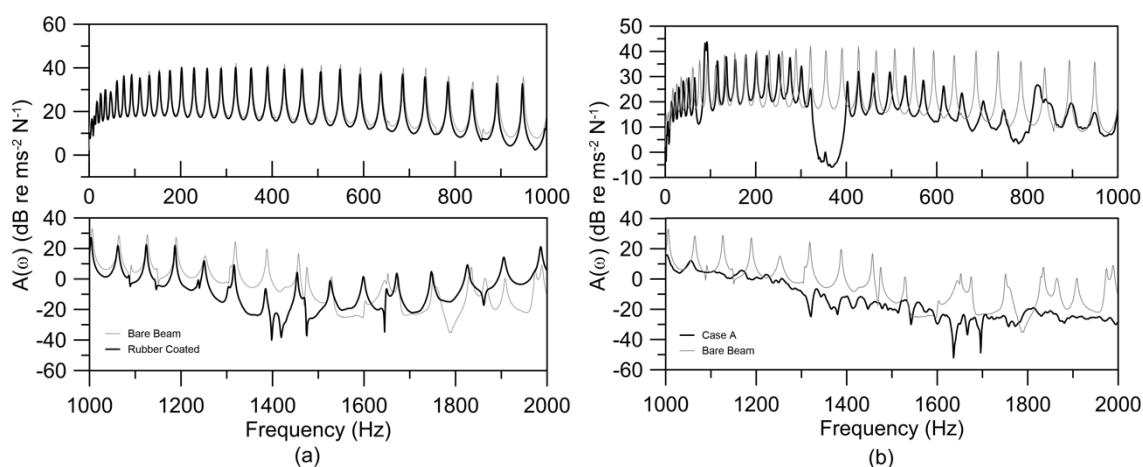


Figure 2. (a) FRFs of the plain beam (grey) and the rubber-coated beam (black). (b) FRFs of the plain beam (grey) and the aluminium beam with eleven magnet pairs (Case A) (black).

It is clear that the increase in mass at each location has increased the depth of the band gap at 350 Hz by approximately 10 dB. The band pass feature at 90 Hz has also been slightly increased and the two minima on either side of the band pass peak are accentuated. At higher frequencies, the signals remain approximately the same except at  $1 \text{ kHz} < f < 1.4 \text{ kHz}$ , where there is some significant attenuation of up to 30 dB. As expected, the increase in mass loading has resulted in a downward shift in the overall frequency of the corresponding peaks.

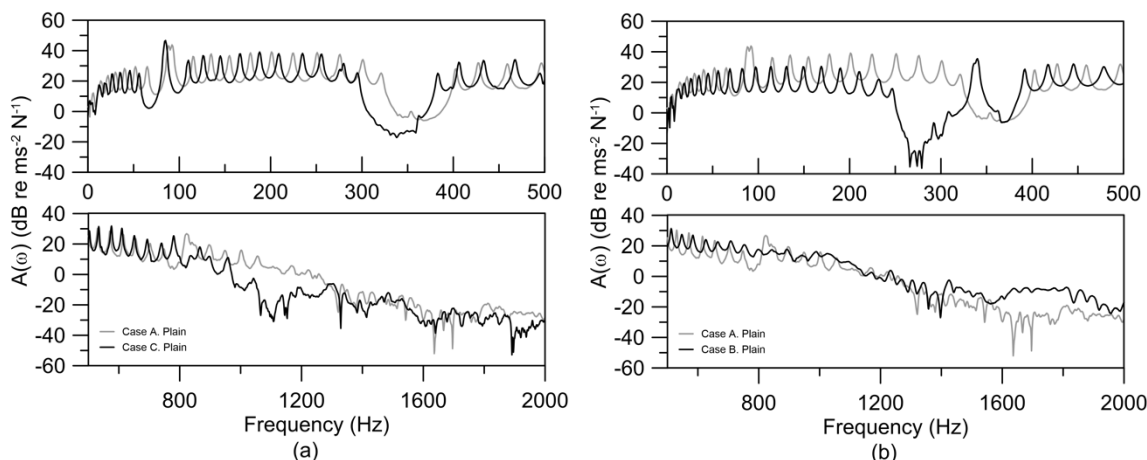


Figure 3. (a) Comparison of the FRFs of Case A (two sets of magnets attached at eleven points, grey) to Case C (four sets of magnets attached at eleven points, black). (b) Comparison of the FRFs of Case A (two sets of magnets attached at eleven points, grey) to Case B (two sets of magnets attached at twenty-two points, black).

Similar results are shown in Figure 3(b) for the comparison between Case A and Case B. In Case B, the spacing between the magnet pairs has been reduced to 182 mm. To achieve this, the total number of magnet pairs was increased from eleven to twenty-two. This meant that the mass at each attachment point was the same for both cases but the total mass loading of the bar was doubled. A clear change in the band gap is observed between 250 and 400 Hz, resulting in a double-band-gap structure in this frequency range as the spatial periodic length is reduced by half. The band pass observed in Case A at 90 Hz is no longer visible. At higher frequencies, the overall level is unchanged up to 1500 Hz, after which Case B displays an increase in level by up to 20 dB.

### 3.2 Rubber-coated aluminium bar with magnets

As mentioned above, the aluminium bar was coated with a thin layer of rubber paint over the entire length and on both sides and the FRFs measured for the same magnet configurations are shown in Figures 3(a) and 3(b). Figure 4(a) shows the FRFs for the plain bar (grey) and the rubber-coated bar (black) up to 2 kHz. As can be seen, below 1 kHz the rubber coating has a minimal effect with only a slight attenuation in the overall signal. For  $1 \text{ kHz} < f < 1.5 \text{ kHz}$ , the rubber results in a larger attenuation; however, for  $1.5 \text{ kHz} < f < 2 \text{ kHz}$ , the amplitude is slightly increased. Generally, the position of the peaks is unchanged over the entire frequency range.

Figure 4(b) shows a comparison of the FRFs of Case A (two sets of magnets attached at eleven points, grey) to Case D (two sets of magnets attached at eleven points with a rubber coating, black). Below 500 Hz, the rubber coating has a minimal effect on the FRF. In the band gap (350 Hz), there appears to be a slight increase in the attenuation (2–3 dB) due to the rubber layer. In the frequency range  $0.8 \text{ kHz} < f < 1.3 \text{ kHz}$ , there is a significant reduction in the amplitude (10–15 dB) but as the frequency increases those effects become more complex.

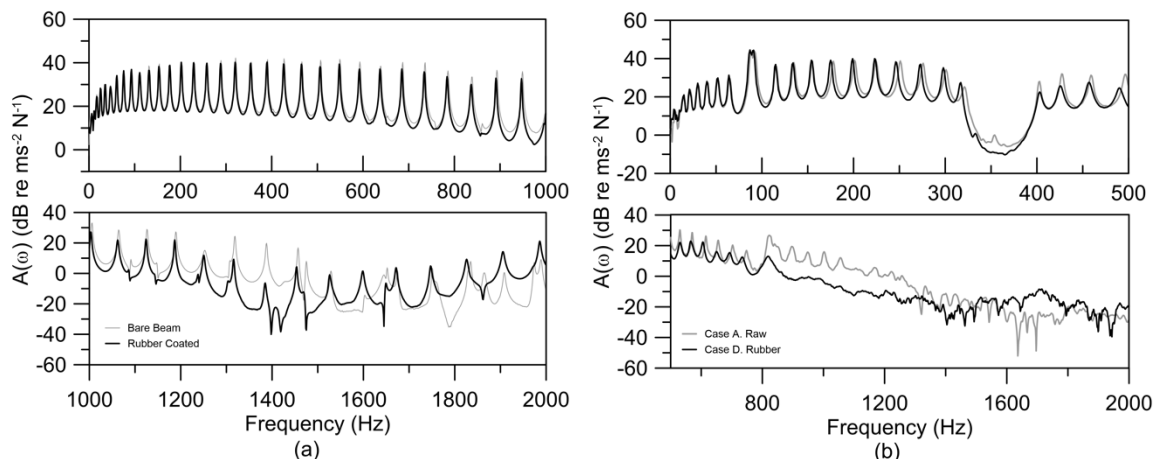


Figure 4. (a) FRFs of the plain beam (grey) and rubber-coated beam (black). (b) Comparison of the FRFs of Case A (two sets of magnets attached at eleven points, grey) to Case D (two sets of magnets attached at eleven points with rubber coating, black).

Similar results were also found for the Cases B–E (two magnets at each location, twenty-two locations) and Cases C–F (four magnets at each location, eleven locations). These are shown in Figures 5(a) and (b), respectively.

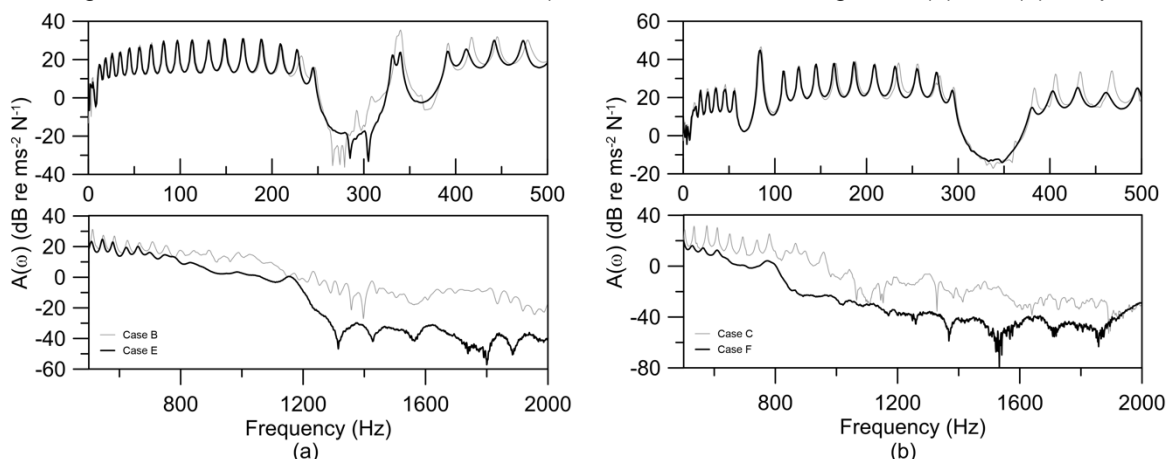


Figure 5. (a) Comparison of the FRFs of Case B (grey) and rubber-coated Case E (black). (b) Comparison of the FRFs of Case C (grey) and rubber-coated Case F (black).

It is clear that the rubber has little effect below 500 Hz, even in the band-pass and band-gap regions. At higher frequencies, however, it results in quite large attenuations (up to 30 dB). This degree of attenuation was not observed in the raw aluminium beam when coated with rubber (Figure 2(a)) and must be attributed to the periodic structures attached to the bar. This experimental observation is different from what was predicted in a study of the effect of a coating on the band-gap properties of an underwater plate with periodically located signal conditioning plates.<sup>[4]</sup> The prediction indicated that, even with a very thin layer of the coating, the “short-circuit effect” of the coating significantly reduces the band-gap properties of the plate. Further work is required to check the conditions used for the current experiment and previous theoretical prediction.

### 3.3 Radiated Sound Intensity

In addition to the surface vibration, the sound intensity was also measured at the same position as the accelerometer, as described in Eq. (1). Comparisons of the various cases listed in Table 1 will be discussed below. Figure 6 shows a comparison of the acceleration and sound intensity for the plain aluminium beam and the rubber-coated bar. The top plots show the acceleration for the entire frequency range  $0 < f < 1000$  Hz while the lower plots show the acceleration (black) and sound intensity (grey) for two regions,  $0 < f < 500$  Hz and  $500 < f < 1000$  Hz. For  $250 \text{ Hz} < f < 600 \text{ Hz}$ , sound intensity has negative values coinciding with the resonance peaks in the acceleration and switches to positive at  $f > 600$  Hz. These results demonstrate the distributed properties of the sound intensity and show that, at certain locations, the sound intensity flow (power per unit area) may flow back to the vibrating structure. Further measurement of sound intensity at other locations on the beam indicated that the sound intensity at the resonance peaks below 600 Hz and near the impact location and middle of the beam could be positive. The total summation of the sound intensity should give the positive overall sound power at all the peak values.

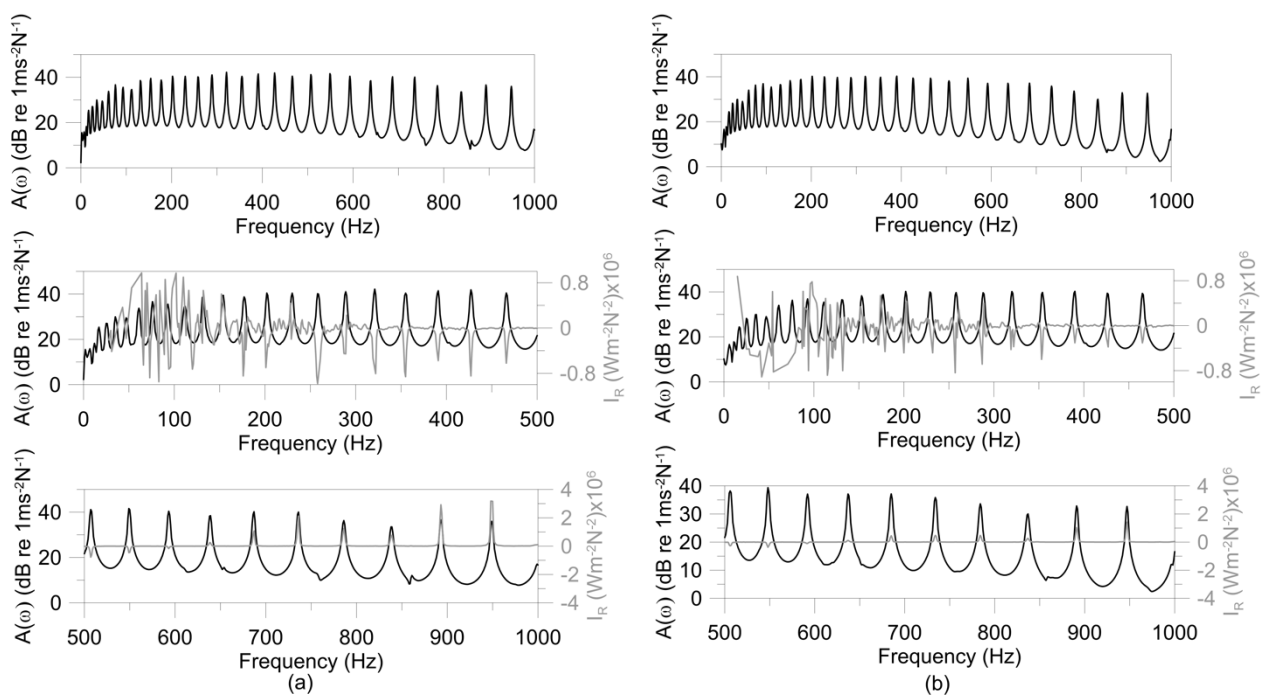


Figure 6. Comparisons of the surface vibration (black) and sound intensity (grey) for (a) the plain aluminium beam and (b) the bar coated with rubber on both sides.

Comparisons of the sound intensity in Figure 6(b) to those in Figure 6(a) show that the rubber reduces the sound intensity at higher frequencies. This is consistent with the reduced vibration of the beam cause by the applied damping at high frequencies.

Figure 7 shows a comparison between Case A and Case D. The two lower plots magnify the two areas of interest, the band pass ( $f \approx 90$  Hz) and the band gap ( $f \approx 350$  Hz). At the band pass peak, the sound intensity shows both positive and negative values, whereas throughout the band gap region the sound intensity is zero. Both of these features are observed in the rubber-coated and plain aluminium bars. Similar results were also observed for Cases C and F with the four magnets. These are shown in Figure 8.

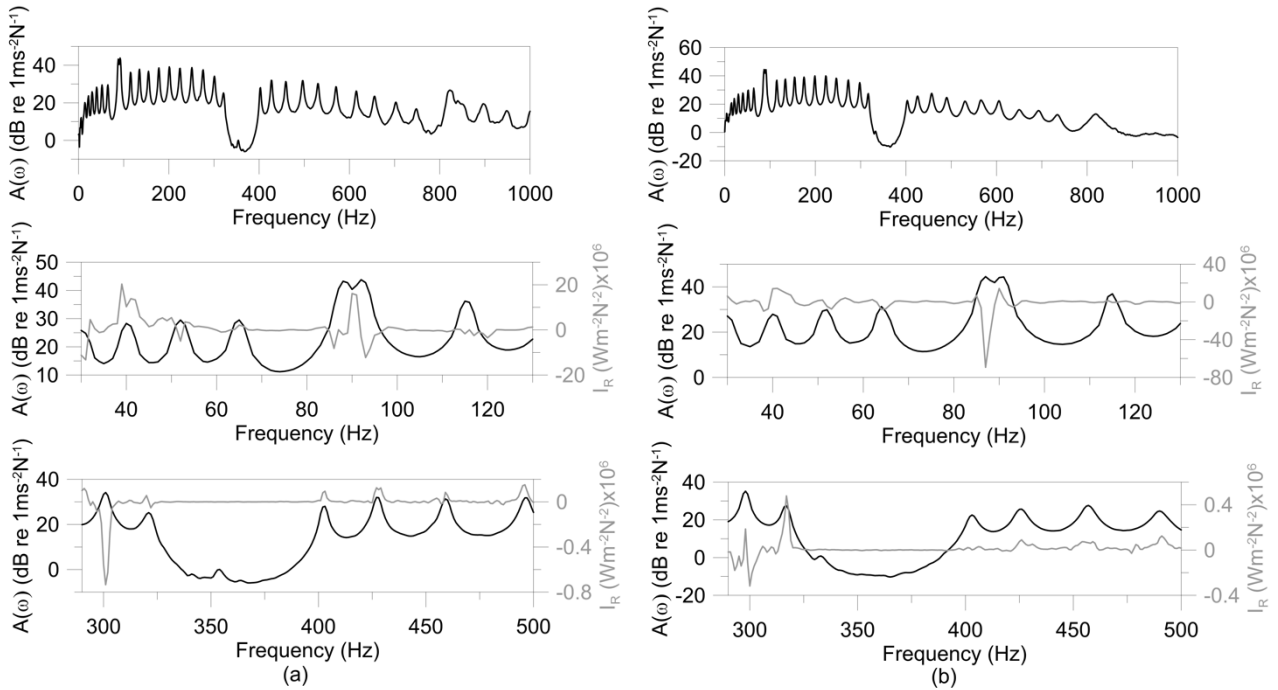


Figure 7. Comparisons between (a) Case A (eleven magnet pairs on aluminium beam) and (b) Case D (eleven magnet pairs on rubber-coated aluminium beam).

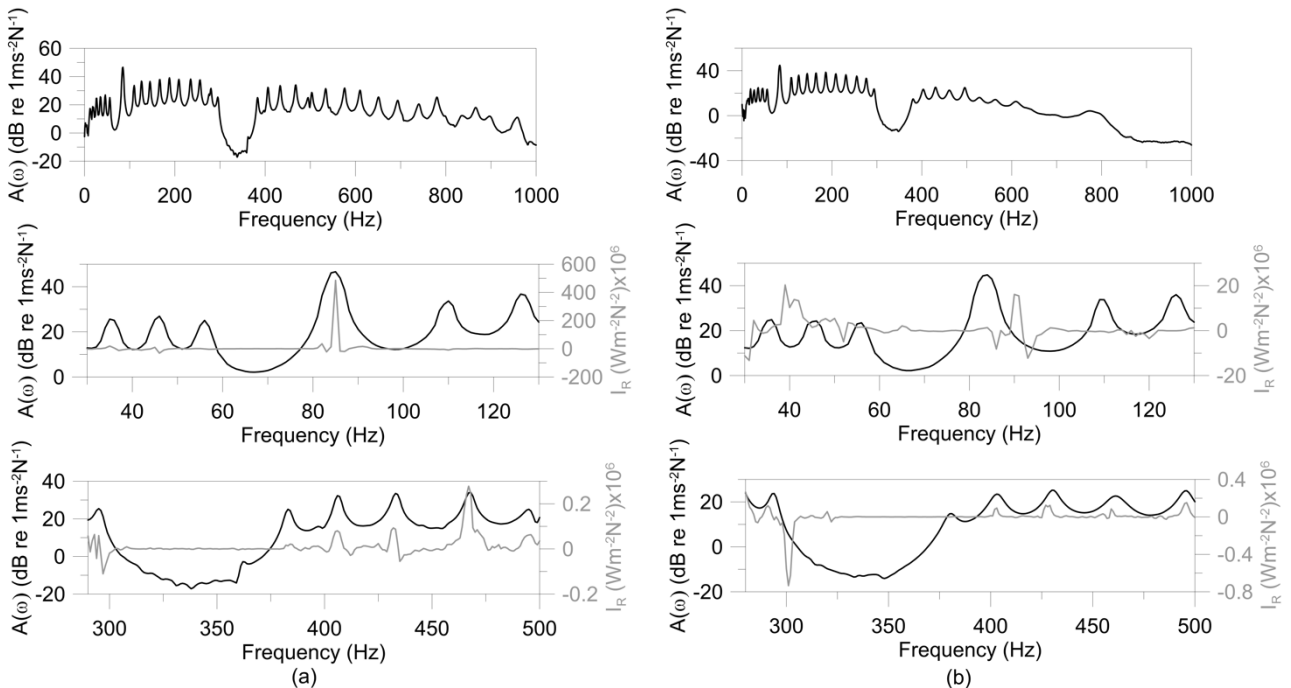


Figure 8. Comparisons between (a) Case C (eleven magnet quads on Al beam) and (b) Case F (eleven magnet quads on rubber-coated aluminium beam).

Figure 9 shows a comparison between Case B and Case E. Once again, the damping of the coating material does not change the band gap properties of the periodic beam. It reduces the peak amplitude and high-frequency structural response as expected.

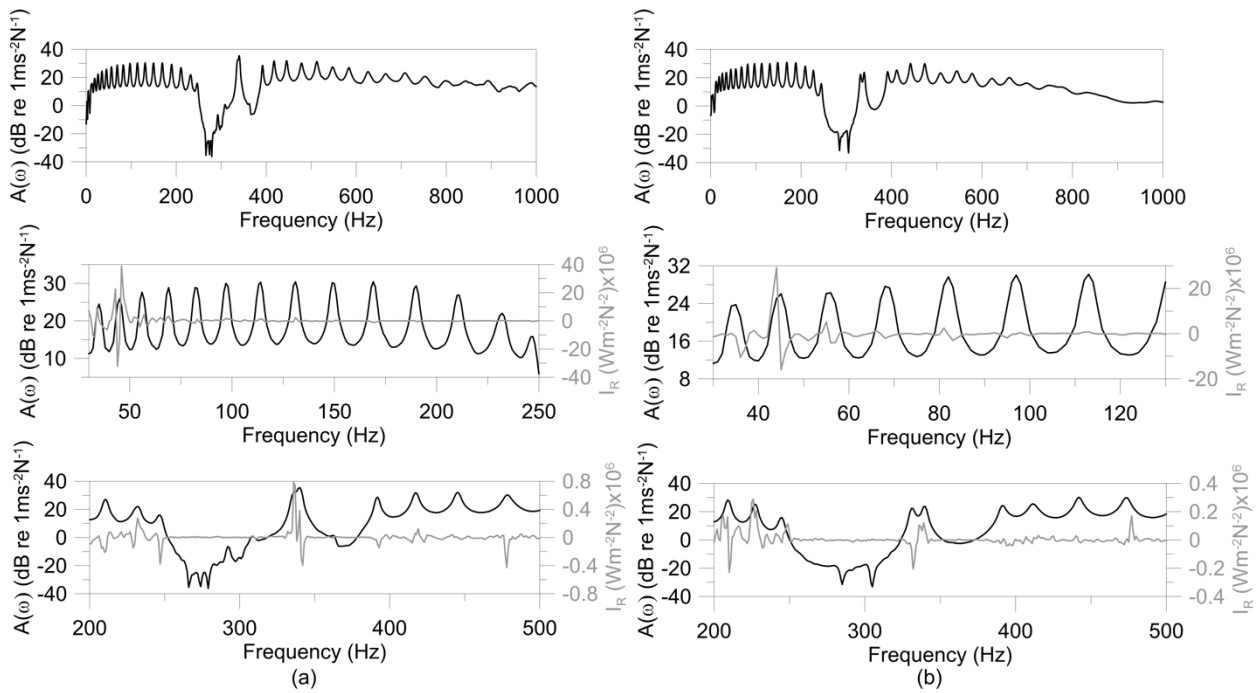


Figure 9. Comparisons between (a) Case B (twenty-two magnet pairs on aluminium beam) and (b) Case E (twenty-two magnet pairs on rubber-coated aluminium beam).

In order to extend this work to a more realistic periodic structure, short aluminium bars were glued directly onto the aluminium beam using polyurethane adhesive. The results are shown in Figure 10. As can be seen, a similar band gap and band pass structure are observed, except at different frequencies and diminished amplitudes. In this case, the band pass is observed around 400 Hz and the band gap around 850 Hz. The results for sound intensity across both regions are similar to those obtained with magnets with fluctuating intensity across the band pass and zero intensity across the band gap.

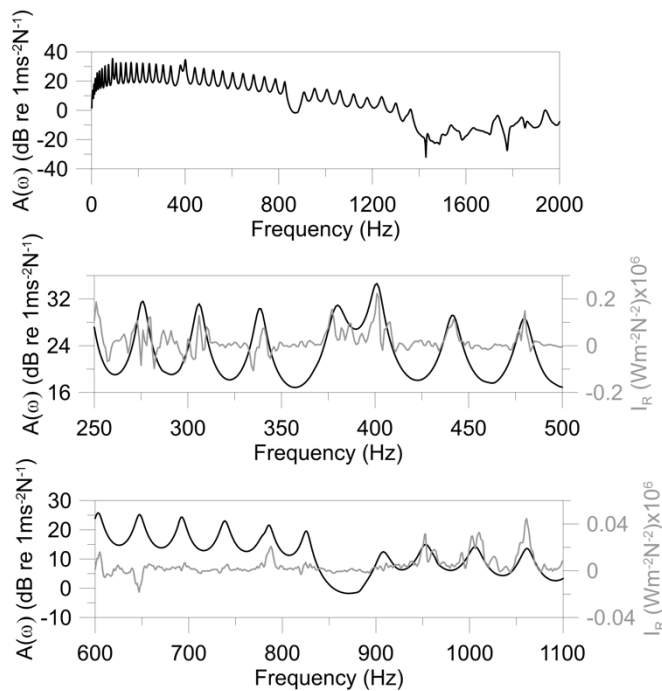


Figure 10. FRFs and sound intensity for the beam with periodically located short aluminium bars.

It is estimated that the first nonzero natural frequency of the short aluminium beam (with free–free boundary condition) is around 470 Hz. However, experimentally, the accelerance of the beam with periodic short aluminium beams did not show any significant variation of the trapped modes associated with this free–free beam mode. A preliminary calculation of the trapped modes generated by the attachment of the short bars to the long aluminium beam shows that the trapped mode is located around 410 Hz and that its effect on the vibration response of the periodic beam is very small. It seems that a detailed modelling of the periodic beam attached with periodically located short beams is necessary so that the effects of the trapped modes on the properties of the periodic beam can be experimentally observable.

#### 4. CONCLUSIONS

An experimental investigation into the vibro-acoustical properties of an aluminium beam attached with periodically located lumped masses and short aluminium bars was undertaken. The band pass and band gap properties of the beam with periodically located masses were observed. The effects of variations in the mass and distance between the masses on the band gap properties were also examined. However, when the beam was attached with periodically located short aluminium bars, only the band gap effect induced by bar's mass was observed. However, the effects of the trapped modes of the short aluminium bars on the band gap properties have not yet been experimentally observed. It is suggested that the optimal length of the short aluminium bar for the effective change of the beam's band gap property via trapped modes should be obtained through a parametric study before further experimental studies can be undertaken.

#### REFERENCES

- [1] Eatwell, G. P., and Butler, D. 1982. "The response of a fluid-loaded, beam-stiffened plate". *Journal of Sound and Vibration* 84 (3), 371–388.
- [2] Mace, B. R. 1980. "Periodically stiffened fluid-loaded plates, I: Response to convected harmonic pressure and free wave propagation". *Journal of Sound and Vibration* 73 (4): 473–486.
- [3] Zhang, Y., Huang, H., Zheng, J., and Pan, J. 2015. "Underwater sound scattering and absorption by a coated infinite plate with attached periodically located inhomogeneities". *Journal of the Acoustical Society of America*. 138 (5): 2707–2721.
- [4] Zhang, Y., Huang, H., Pan, J. 2017, "Underwater sound radiation from an elastically coated infinite plate with periodic inhomogeneities of finite width." *Journal of the Acoustical Society of America*. 142(1), 91–102.
- [5] Zhang, Y., and Pan, J. "Enhancing acoustic signal response and absorption of an underwater coated plate by embedding periodical inhomogeneities". *Journal of the Acoustical Society of America*. submitted.